

Ore Deposits Research Section
The Pennsylvania State University
University Park, PA 16802

Can the contract
be continuing

A Report on the Project

**PREPARATION FOR KINETIC MEASUREMENTS ON THE
SILICATES OF THE YUCCA MOUNTAIN POTENTIAL REPOSITORY**

to

Los Alamos National Laboratory
June 15, 1993 to September 30, 1993

RECEIVED
AUG 19 1994
OSTI

Part I. The Preparation Of Clinoptilolite, Mordenite And Analcime

Rick

H. L. Barnes and R. T. Wilkin

INTRODUCTION

This report summarizes progress made during the contract period on preparing Na-end member clinoptilolite, mordenite, and analcime. The objective is to use the prepared zeolites during the next contract period to determine rates of dissolution and precipitation in laboratory flow-through systems in both our lab to 350°C and by the geochemists at Yale University to about 80°C. Because clinoptilolite represents the most complicated phase of these three zeolites and it is most abundant at Yucca Mountain, we have concentrated most of our efforts on its preparation. Initially, we explored the possibility of synthesizing pure Na-clinoptilolite; however, this approach, as discussed in detail in the body of the report below, has proven to be less effective for the several hundred grams needed than to treat selected natural materials. Consequently, we have searched for, and have since collected, high-concentration (about 95%) natural

MASTER

DISTRIBUTION OF THIS DOCUMENT IS UNLIMITED

YPR

DISCLAIMER

**Portions of this document may be illegible
in electronic image products. Images are
produced from the best available original
document.**

clinoptilolite samples. To further concentrate the natural samples which contain ~5-10% impurities mostly of smectite, a hindered settling technique that takes advantage of the relatively low specific gravity of clinoptilolite coupled with ultrasonic cleaning in de-ionized water has been employed. X-ray powder diffractometry and SEM analysis of the concentrated zeolite indicates that a purity of >99% can be achieved for the needed quantities. This material is now a mixed Na-K zeolite which must then be converted to the pure Na-end member composition. Published work by Pozas *et al.* (1989) and Liang and Sherriff (1993) indicates that the desired composition approaching Na-clinoptilolite can be prepared by hydrothermal cation exchange treatment. By adopting their methods, we anticipate that the necessary end member starting materials will be ready in sufficient quantities so that the kinetic studies can proceed without delay beginning with the next fiscal year contract.

*borderline
amorphous
containing
clay*

MATERIAL REQUIREMENTS

For the initial series of kinetic experiments, we plan to use the NA-end members of the zeolite solid solutions before dealing with the other alkali elements. Consequently, we require ~500g of pure Na-zeolites that are well crystallized (>10 μm) and devoid of sharp edges or high defect concentrations that carry excess surface energy.

*non-uniform
of natural
minerals*

SYNTHESIS OF ZEOLITES

There are few descriptions in the literature of methods for clinoptilolite synthesis (e.g., Chi and Sand, 1983). The methods that have been described typically yield other undesirable phases and do not provide a significant advantage over natural samples. However, a method was developed following a procedure that has proven to be successful for kaolinite (G. Kakandes, pers. comm.). In summary, organic-based Al (Al-

isopropoxide) and Si (tetraethyl orthosilicate) are heated and mixed in stoichiometric proportions with NaOH to form a homogeneous melt. The melt is hydrated to form a gel which is then dried to form a powder. The powder (~50 mg) is sealed in a glass reaction tube (3 mm I.D. x 10 cm) with excess water and heated to 250°C to crystallize clinoptilolite. This method differs from other methods in that the elements are mixed prior to gel formation; whereas, in the Ludox-based method of Chi and Sand (1983) the elements are added to a pre-existing silica gel. These other methods do not allow for intimate mixing of the elements, and thus, result in the formation of undesired accessory phases.

In the adopted method, the sealed glass reaction tubes were periodically (every ~120 hr) removed from a vertical tube furnace. The tubes were opened and the contents filtered, ground, washed with de-ionized water, and finally, analyzed by X-ray powder diffractometry with Ni filtered $\text{CuK}\alpha$ radiation, scanning from 5-60 degrees 2θ at $2^\circ \theta$ per minute. These experiments, however, yielded mixed results. Clinoptilolite was not produced as a single phase. Instead the products consisted either of a mixture of analcime and albite, or crystallization was incomplete and a broad amorphous hump was observed on the diffraction patterns. The lack of success with these initial experiments provided the impetus to obtain natural samples; however, continuing testing of this method will include varying of temperature (125°C), run duration, and perhaps the addition of clinoptilolite seeds.

In contrast to clinoptilolite, there is a considerable literature dedicated to the synthesis of mordenite (e.g., Bajpai, 1986). Very recently, a straightforward technique has been described by Hurem *et al.* (1993). This method is reported to produce single phase mordenite with variable molar ratios of $\text{SiO}_2/\text{Al}_2\text{O}_3$ of 10-30 depending on crystallization conditions. We shall test and probably adopt this method for the preparation of the

large port vs small port
unreacted material

need ~1 g
of pure sample
(at least 0.3 g)

needed quantities of mordenite. In addition, we expect that by varying the relative proportions of elements in the above method for clinoptilolite synthesis, that pure analcime may be produced readily and as a useful alternative to finding and cleaning natural samples.

NATURAL ZEOLITES

Natural clinoptilolite samples have been obtained from Steelhead Specialty Minerals, Spokane, WA. The purity of this material in the 10-30 μ m size fraction, as determined by X-ray powder diffractometry and SEM analysis, is greater than ~90%. In addition, clinoptilolite samples from Buckhorn, New Mexico; Castle Creek, Idaho; Mud Hills, Idaho; Sheaville, Oregon; and Shoshone, California have been collected. These later samples have been the focus of on going studies of zeolite beneficiation and ion exchange capacity by F.F. Aplan of the Mineral Processing Section at Penn State University. For this project, we have taken advantage of his group's research. The mineralogic composition of the sampled sedimentary zeolite deposits is presented in Table 1. Typical impurity accessory phases in sedimentary zeolite ores include quartz, microcline, ^{pyro}_{nat}, montmorillonite, and glass. Note the exceptional purity of the Castle Creek deposit (~95%). Figure 1 shows SEM photomicrographs of clinoptilolite from the Castle Creek deposit where the clinoptilolite is in the form of euhedral crystals up to ~20 μ m in size. Clinoptilolite from this deposit is enriched in Na₂O (4.80 wt.%) relative to K₂O (1.42 wt.%) (Mondale *et al.*, 1988).

Several methods have been tested in trying to remove impurities from the natural clinoptilolite concentrates. Centrifugation proved to be adequate but inefficient as only small quantities of material could be processed at one time. A hindered settling technique was developed and applied to the sample from Steelhead Specialty Minerals Company.

TABLE 1. Mineralogic composition of several sedimentary zeolite deposits

	Clinoptilolite (%)	Quartz (%)	Montmorillonite (%)	Glass (%)	K-spar (%)	Mordenite (%)	Calcite (%)
Clinoptilolite							
Buckhorn, NM	91	5		2	2		
Castle Creek, ID	95		5				
Mud Hill, CA	90	7		3			
Sheaville, OR	92	1		5	1		1
Shoshone, CA	91	1		5		1	2
Mordenite							
Copper Valley, NV	10	5	4		1	85	

Note: Data from Mondale (1978) and Carland (1980) where percentages were determined by particle counting in transmitted light. We have obtained ~2kg splits of the samples described by these authors.

wow!
low
detection
limits

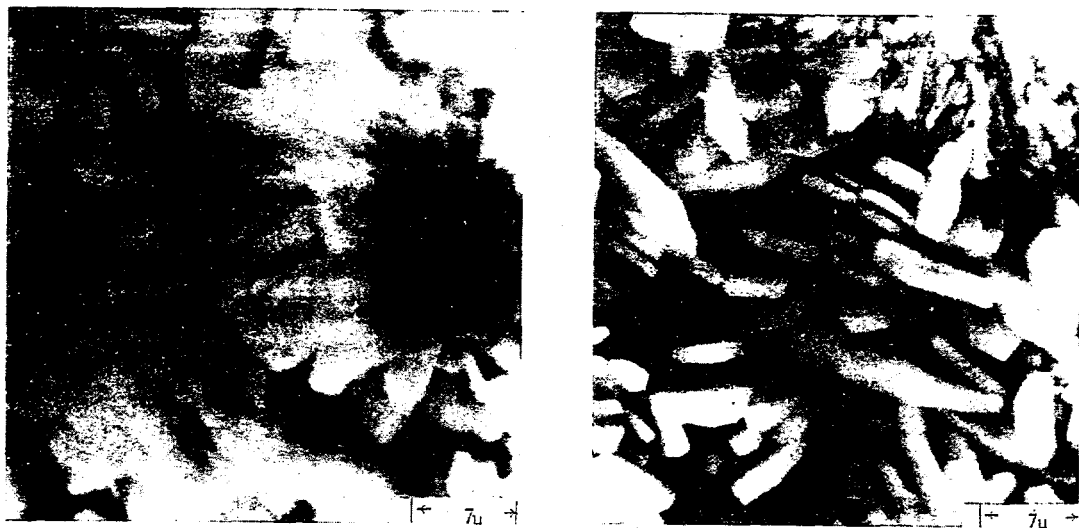


Figure 1. SEM photomicrograph of foliated aggregates of clinoptilolite crystals from Castle Creek, ID (*from* Mondale, 1978).

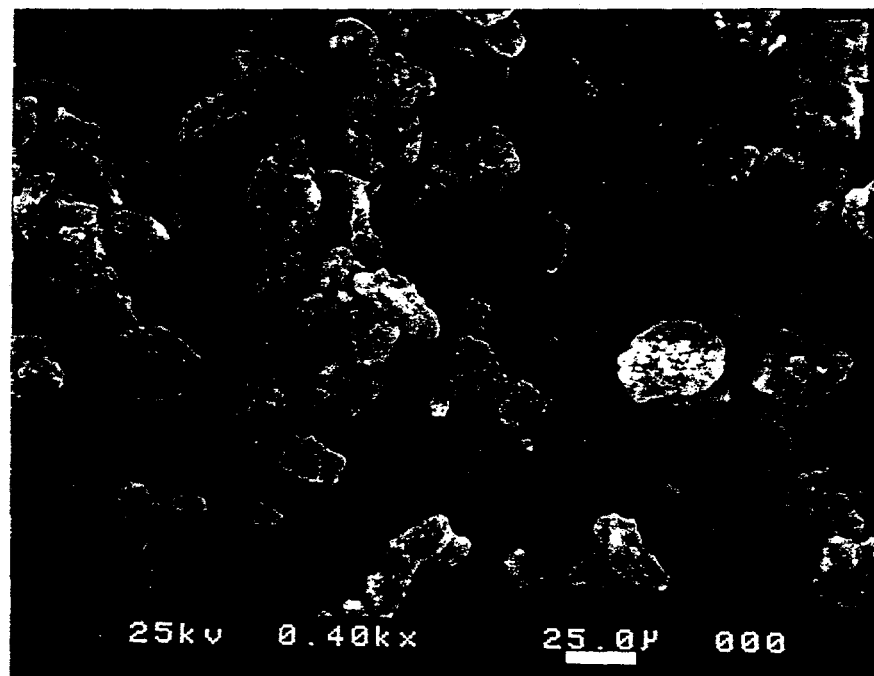


Figure 2. SEM photomicrograph of clinoptilolite ore obtained from Steelhead Specialty Minerals after concentration/ultrasonic treatment.

Approximately 15 g of a -30 mesh clinoptilolite concentrate was placed in a 1 L cylindrical, separatory funnel. Tap water was flowed into the bottom of the funnel at a slow rate, the rate of flow being gradually increased until a clear separation was observed with the heavy particles left at the bottom of the funnel. The suspended material was then transferred to a 1 L graduated cylinder, covered and allowed to settle overnight. The overlying suspension was then siphoned off; the sediment mixed with de-ionized water in a beaker and cleaned in a ultrasonic bath for 1 hour, changing the cleaning solution every 10 minutes. The concentrate was dried at 60°C overnight in an oven. SEM study shows the mineral surfaces are free of ultrafine particles (Fig. 2). X-ray powder diffraction and particle counting using SEM scanning indicates that the final concentrate is greater than 99% clinoptilolite. Approximately 500 g of this material has been processed.

A mordenite-bearing sample from Copper Valley, NV has also been collected (Table 1). Because the sample contains a significant amount of clinoptilolite (~10%) that is not readily separable, mordenite will have to be synthesized.

PRESENT STATUS OF THE ZEOLITE PREPARATIONS

We only recently received and began processing the clinoptilolite samples listed in Table 1 to find if the concentrates made, especially from the Castle Creek sample, are superior to that from the material from the Steelhead Specialty Minerals Company. After the concentrating process is completed, cation exchange will be carried out at 60°C in solutions of 2 M NaCl and 1 M NaOH (10g solid/1L solution). The solutions will be replaced daily and a portion of the solid will be collected for major element analysis by ICP spectroscopy. By this regular sampling and analyses, the change of Na₂O/K₂O in the clinoptilolite can be followed through time until the product becomes satisfactorily close

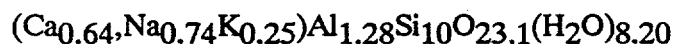
long process

to the pure end member. We also will examine the cation-exchanged minerals by microprobe techniques to evaluate grain homogeneity.

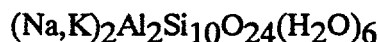
Besides the clinoptilolite that is being prepared in large quantities, we have on hand 5.8 g of carefully hand picked material from Succor Creek in addition to the 0.9 g which we have supplied to Yale for initial experiments. It has been analyzed in our Materials Characterization Laboratories and has the following composition:

L.O.I.	39.6 mole percent
SiO ₂ ,	48.3
Al ₂ O ₃	6.17
TiO ₂	<0.01
Fe ₂ O ₃	0.02
MnO	0.01
CaO	3.10
MgO	0.35
Na ₂ O	1.80
K ₂ O	<u>0.61</u>
Total	99.96

and the composition, normalized on silica and taking the loss on ignition as water, of:



compared to the nominal composition of:



Although the preparation of clinoptilolite is apparently resolved, more experiments are necessary to complete the design of methods for syntheses of both mordenite and analcime. For this reason, there are underway now further experiments on mordenite synthesis..

REFERENCES CITED

Bajpai, P.K. (1986) Synthesis of mordenite type zeolite: *Zeolites*, 6, 2-8.

Bish, D.L. (1984) Effects of exchangeable cation composition on the thermal expansion/contraction of clinoptilolite: *Clays and Clay Minerals*, 32, 444-452.

Carland, R.M.P. (1980) Studies of cation exchange properties in natural sedimentary zeolites: M.Sc. thesis, The Pennsylvania State University, University Park.

Chi, C. and Sand, L.B. (1983) Synthesis of Na- and K- clinoptilolite end members: *Nature*, 304, 255-257.

Hurem, Z., Vucelic, D., and Markovic, V. (1993) Synthesis of mordenite with different $\text{SiO}_2/\text{Al}_2\text{O}_3$ ratios: *Zeolites*, 13, 145-148.

Liang, J. and Sherriff, B.L. (1993) Lead exchange into zeolites and clay minerals: A ^{29}Si , ^{27}Al , ^{23}Na solid state NMR study: *Geochim. et Cosmochim. Acta*, 57, 3885-3894.

Mondale, K.D. (1978) The characterization, beneficiation and ion exchange properties of natural sedimentary zeolites: M.Sc. thesis, The Pennsylvania State University, University Park.

Mondale, K.D., Mumpton, F.A., and Aplan, F.F. (1988) Properties and beneficiation of natural sedimentary zeolites: *In Process Mineralogy VIII*, edited by D.J.T. Carson and A.H. Vassiliou, The Minerals, Metals, & Materials Society, pp. 249-275.

Pozas, C., Quintanilla, D.D., Parienta, J.P., Molharbe, R.R., and Magi, M. (1989) Hydrothermal transformation of natural clinoptilolites to zeolites Y and P1: Influence of the Na, K content: *Zeolites*, 9, 33-39.

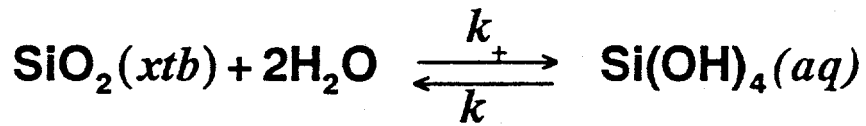
Part II. Draft Manuscript on the Heterogeneous Kinetics of Cristobalite

Precipitation and dissolution rate constants for cristobalite at 150-300°C

P. J. N. Renders¹, H. L. Barnes, and C. H. Gammons²

Ore Deposits Research Section, The Pennsylvania State University,
University Park, PA 16802, U.S.A.

Abstract-- Experiments on the rates of reactions of dissolution and precipitation of cristobalite



were carried at 150-300°C. The rate constant for precipitation in pure water is given by

$$\ln K_- = -2.248 - \Delta E_a / R^*(1/T), \text{ in kilojoules and kelvins.}$$

The energy of activation, ΔE_a , is 50.0 ± 2.4 kJ/mol. These results show that cristobalite may precipitate from hydrothermal solutions if the concentration of Si(OH)_4 exceeds that at quartz saturation and is less than that of amorphous silica saturation and if there are cristobalite nuclei present. Such nuclei may occur where there has been devitrification of volcanic glasses, for example. Cristobalite has refused to crystallize in the absence of such nuclei. See, p. 14

Steady state concentrations were reached experimentally after starting at 150° with initially supersaturated solutions and at 200°C starting with either supersaturated or undersaturated solutions. From the steady state conditions, equilibrium constants can be derived for the above reaction: $pK_{150} = 2.22$ and $pK_{200} = 2.10$, values in close agreement with published data.

¹Now at the Department of Geological Sciences, State University of New York at Albany.

²Now at the Department of Geological Sciences, McGill University, Montreal, Quebec.

Introduction

Kinetic data for quartz, cristobalite, and amorphous silica are necessary to model the presence or absence of these phases under varying conditions of temperature, pressure, and chemistry. While quartz is the stable silica polymorph under the conditions investigated here, which silica polymorph precipitates from solution depends on kinetic in addition to thermodynamic constraints.

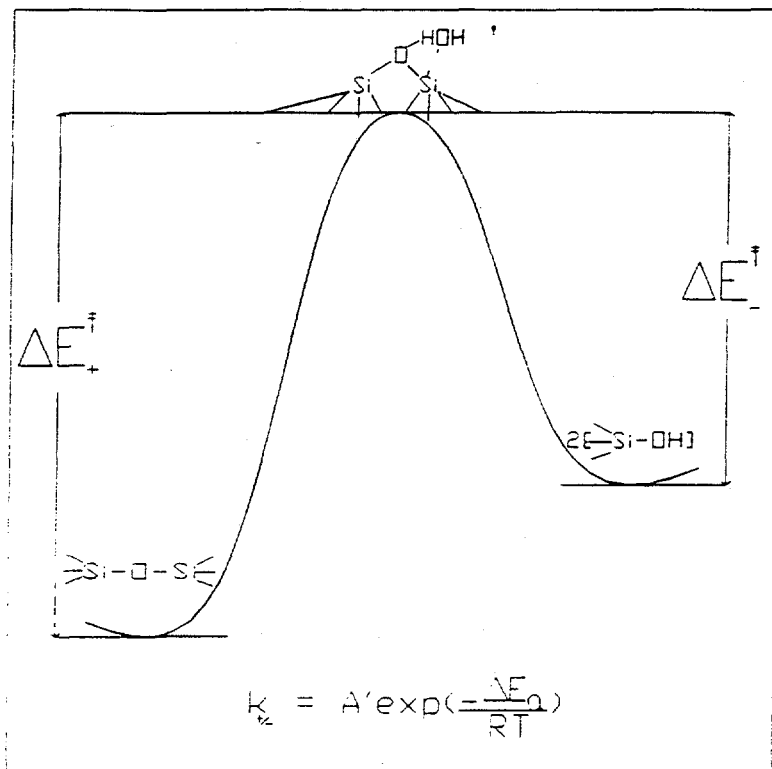
Examples of systems in which non-equilibrium silica precipitation may occur include; the formation of sinter terraces associated with hot springs, scaling in geothermal energy wells e.g. Wairakei geothermal fields, active hydrothermal systems especially associated with volcanics where cristobalite is in contact with aqueous fluids from temperatures of 25° to 180°C (FOURNIER, 1973 and JACKSON et. al. 1977), and silica dissolution and precipitation induced by localized temperature increases (<200°C) such as would be associated with nuclear waste burial.

The primary objective of this research then was to determined precipitation and dissolution rate constants for cristobalite over the temperature range 150° to 300°C. In addition, this work was undertaken to gain further insight into the microscopic processes involved in the hydrolysis of a silica pure phase.

Although kinetic data for quartz from 25° to 300°C are available, there is relatively little experimentally based, kinetic data for amorphous silica and none for cristobalite. Dissolution rates for quartz in pure H₂O have been measured from 200° to 300°C by DOVE and CRERAR (1990) and 70°C by KNAUSS and WOLERY (1988). RIMSTIDT and BARNES (1980) derived rate constants from precipitation and dissolution experiments in pure H₂O for quartz and amorphous silica from 18° to 305°C.

It has been stated, RIMSTIDT and BARNES (1980), that the precipitation mechanism (on the molecular scale) of all silica polymorphs is the same and therefore their precipitation rates should also be the same for a given temperature and pressure. (According to transition state theory (EYRING 1935), the rate of a precipitation reaction is directly proportional to the energy (ΔE^f) needed to form the intermediate or activated complex. As Si(OH)₄ is the reactant in the precipitation of all SiO₂(s) polymorphs under hydrothermal conditions of interest here the activated complex and ΔE^f must be the same for all silica precipitation reactions, Fig. 1.)

While the results presented do not support the prediction of equivalent precipitation rates, RIMSTIDT and BARNES (1980), for different SiO₂ polymorphs, they do suggest operation of the same rate limiting step in the precipitation of quartz, amorphous silica and

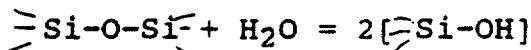


Reaction Coordinate

Figure 1. Schematic, modelling the formation of an activated complex during one of a series of elementary reactions leading to the separation/attachment of an orthosilicic acid molecule from/to the SiO_2 ,_s polymorph surface. The rate of separation/attachment as quantified by the rate constant k is proportional to E .

cristobalite. This conclusion is based on the similar activation energies for cristobalite precipitation determined here ($50.0 \pm 2.4 \text{ kJ}\cdot\text{mol}^{-1}$) with those for quartz 51 to $55 \text{ kJ}\cdot\text{mol}^{-1}$ (BIRD et al., 1986) and quartz and amorphous silica ($49.8 \text{ kJ}\cdot\text{mol}^{-1}$) determined by RIMSTIDT and BARNES (1980).

Evidence is also presented which strongly suggests that cristobalite will precipitate directly from aqueous solution as a metastable silica polymorph if cristobalite substrate is present and total molal aqueous silica ($\text{mSi(OH)}_4, t$) is greater than total molal aqueous silica corresponding to cristobalite saturation ($\text{mSi(OH)}_4, x_{\text{tb}}$). Given that equivalent rate constants for cristobalite were derived from dissolution and precipitation measurements the rate of both processes was shown to be controlled, under conditions of near neutral pH, by an elementary reaction of the type.



Where sequential additions of H_2O molecules to the silica substrate result in the formation of the aqueous silica species Si(OH)_4 .

Experimental Method

X Synthetic cristobalite, ground with a mortar and pestle and sieved to collect the -100 to +400 mesh fraction, was used in all experiments. The sieved fraction was cleaned ultrasonically in distilled water to remove ultra fines (the ultra sonic cleaning rapidly dissolves high energy sites on the cristobalite seed material). SEM photographs before and after cleaning confirmed the absense of ultra fines and sharp edges on the seed material. BET Surface area measurements were made using N_2 as the adsorbate. The actual specific surface areas for the different batches of run material are listed in Table (1). *See drawing*

Three Phase Experiments

The initial dissolution experiments were conducted along the liquid-vapour curve of the solution in a 0.360 l titanium alloy (Ti-17) autoclave. Approximately 0.2 kg of freshly boiled water was weighed into the evacuated autoclave containing a known mass of cristobalite seed material. The vessel was then heated to the desired run temperature (which was achieved in under 6 hours).

Samples were obtained from the autoclave through a length of coiled 1/16" O.D. stainless steel capillary tubing immersed in an ice-water bath. By quenching the sample, precipitation of silica in the sampling tube, was eliminated due to very slow $0^\circ C$ precipitation rates. Weighed samples

Table 1. Experimental data for the precipitation rate of cristobalite.

T°C	pK _{eq} ¹	pK _{eq} ²	Net Reaction direction	A/M (m ² /kg)	log k
150	2.37	2.22	(-)	1.6	-6.55
150	----		(+)	1.2	-6.49
200	2.12	2.10	(-)	0.9	-5.96
200	2.11		(+)	0.55	-5.92
	2.12		(+)		-----
210	2.08		(+)	1.4	-5.78
250	1.92		(+)	1.4	-5.55
300	1.75		(+)	0.15	-4.91
300	----		(+)	1.4	-5.18

1 linear regression of Fournier and Rowe (1962) pK vs. 1/T data.

2 values determined by approach to steady state conditions this study

were stabilized with ultra pure HF for analysis (along with blanks treated in an identical manner) by DCP emission spectroscopy.

For experiments above 250°C the increasing length of time required for the autoclave to stabilize reduced the sampling interval necessary to obtain a minimum of three samples having having a maximum variation in $mSi(OH)4$, and $mSi(OH)4,t$, less than $mSi(OH)4,qtz$. A modified experimental approach, where the runs were conducted at above ambient pressures, was devised which reduced the initial thermal stabilization time to less than 30 minutes. Although the modified procedure was designed specifically for higher temperature runs it had a number of additional advantages over runs along the liquid vapour curve of the system (which are discussed later) and thus was used for all subsequent runs.

Two Phase Experiments

For the remaining experiments a 1.2 l autoclave, used as a pressure ballast and solvent reservoir, was connected to the Ti-17 autoclave by stainless steel capillary tubing as shown in Fig. 2. The evacuated Ti autoclave, containing a known mass ($\sim 10^{-3}$ kg) of cristobalite, was heated to the desired run temperature minus 50°C. The solvent reservoir was then opened to the Ti autoclave, filling the autoclave in less than one minute. The reservoir, still open to the Ti

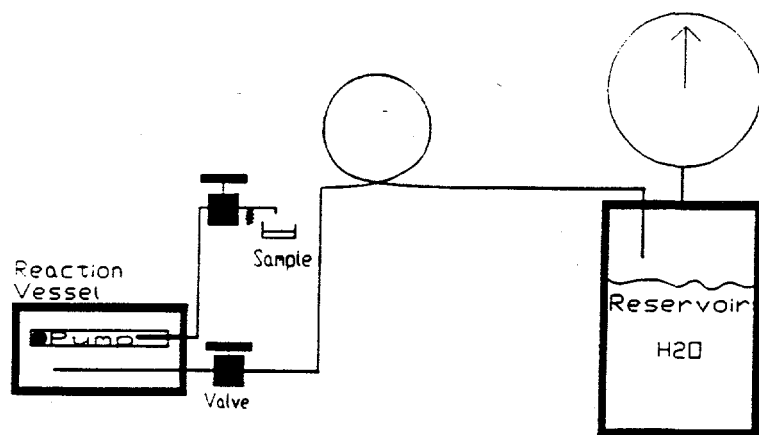


Figure 2. Diagram of the two phase experimental apparatus. Reaction vessel contained only solid and liquid phases under run conditions.

autoclave was finally heated to 350°C generating a total pressure of 165 bars during each experiment.

This procedure significantly reduced the time to achieve temperature equilibrium thereby enabling the attainment of dissolution and precipitation concentration-time data (by filling the reaction vessel with aqueous silica solutions) far from equilibrium especially at temperatures above 200°C. As these experiments were conducted with the reaction vessel containing only solid and liquid phases one further modification (to the original experimental methodology) was required to provide adequate mixing of the contents. A 2.5 cm I.D. 316 stainless steel tube the length of the Ti-17 autoclave's inner chamber was suspended within the reaction vessel. A 2.5 cm diameter 316 stainless steel ball bearing placed inside the tube would roll from end to end of the tube during rocking of the autoclave which circulated the run fluids without damaging the seed material.

Changes in the A/M ratio in these two phase experiments were significantly reduced (A the solid's surface area and M the mass of solution are normally assumed to be constant in heterogeneous rate experiments.) While the value of A would be effected by dissolution to the same extent in these experiments¹ M decreased with each sampling episode during the early experiments while M was a constant in the latter

¹ The worst case was 14% decrease in area at 300°C which is within the uncertainty of the determined rate constants.

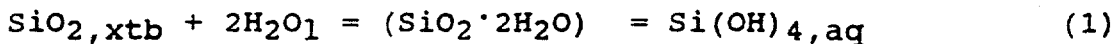
runs.

The total mass of solution in the Ti autoclave was calculated from the autoclave's known 25°C volume and the density of H₂O at the temperature of interest. Samples were taken as previously described with solution transfer from the reservoir arrested during sampling. The transfer of H₂O to the reaction vessel after sampling diluted the reacting silica solution by a known amount (the sample mass) and therefore multiple sampling events no longer generated cumulative uncertainties in the calculated rate constant.

Analysis of experimental data

Rate constants were extracted from the experimental data following the method and theory described in RIMSTIDT and BARNES (1980) and LASAGA (1981). A condensed discussion of the key equations and assumptions used in their interpretation follows.

The overall reaction used to describe the dissolution and precipitation of cristobalite was



where $(\text{SiO}_2 \cdot 2\text{H}_2\text{O})$ represents all intermediate steps between the solid and aqueous silica state. (The actual rate limiting elementary step being measured is undetermined, yet it is thought to be one of a series of sequential reactions occurring between hydroxyl and silicon ions in transition from SiO_2, xtb to Si(OH)_4 and therefore a measurement of the overall rate is also a measurement of the rate limiting step.) It is assumed that Eqn (1) described a reversible reaction, i.e. the rate determining elementary reaction being the same in either direction. This assumption is fundamental to the data treatment followed and is supported by the results obtained.

The net rate of reaction for Eqn. (1) is the sum of the dissolution and precipitation rates:

$$\frac{dm}{dt} \text{Si(OH)}_4, \text{aq} = \left(\frac{A}{M} \right) (k_{+a} \text{SiO}_2 \cdot 2\text{H}_2\text{O} - k_{-a} \text{Si(OH)}_4) \quad (2)$$

where P , T , M , $\alpha_{\text{Si(OH)}_4}$ are constant and

$\frac{dm_{\text{Si(OH)}_4}}{dt}$ = reaction rate ($\text{mol m}^{-2} \text{ s}^{-1}$) for the Si(OH)_4 ion

A = liquid solid interface (m^2)

M = mass of solution (kg)

a_i = activity of the i^{th} component

k_- = precipitation rate constant

k_+ = dissolution rate constant

and the standard states chosen were a hypothetical 1 molal aqueous solution, the pure solid, and pure liquid at the temperature and pressure of interest.

For a system at equilibrium dm/dt = zero and by rearranging Eq (2) the thermodynamic equilibrium constant K_{eq} can be seen to be equal to

$$K_{\text{eq}} = k_+ / k_- \quad (3)$$

Rearranging (3) and substituting for k_- in (2) results in

$$\frac{dm_{\text{Si(OH)}_4, \text{aq}}}{dt} = \left(\frac{A}{M} \right) k_+ a_{\text{SiO}_2} a_{\text{H}_2\text{O}}^2 (1 - Q/K_{\text{eq}}) \quad (4)$$

where Q is the activity quotient of the system and the ratio Q/K_{eq} defines the degree of saturation of the system.

For these experiments interpretation of the data was carried out by deriving the integral of Eqn (4)

$$t = - \left(\frac{M}{A} \right) 1/k \ln \left((1-Q/K_{eq}) / (1-Q_0/K_{eq}) \right) \quad (5)$$

which is the equation of a straight line having a slope equal in magnitude to the precipitation rate constant. Finally precipitation and dissolution rate constants were derived from batch dissolution and precipitation experiments using Eqns (3) and (5).

With the rate constants for Eqn (1) determined, the activation energy of the rate limiting elementary step was obtained using an Arrhenius equation

$$\ln k = \ln A' - E_a / R \cdot (1/T) \quad (6)$$

in which A' is a pre-exponential factor proportional to the entropy of formation for the activated complex, the activity coefficients of the reactants and products,

$$A' = \frac{kT}{h} \frac{O_r}{O} \cdot \exp \cdot \exp \frac{-S}{R} \quad (7)$$

and the fundamental frequency kT/h . (For an in depth discussion of the pre-exponential factor see LASAGA, 1981 and DOVE and CRERAR, 1990.)

Results

Precipitation rate constants determined from net rate measurements in deionized water over a temperature range of 150° to 300°C are summarized in Table 1 and illustrated by the Arrhenius plot, Fig. 3. Figures 4 and 5 illustrate changes in mSi(OH)_4 vs. time from initially under and over saturated solutions (with respect to cristobalite). Figures 6 and 7 illustrate Q/K_{eq} vs. time data from which values of k_+ were derived.

The assumption inherent in the derivation of k_- and k_+ from the experimental data is that the precipitation and dissolution of cristobalite both proceed through identical rate controlling elementary steps. Values of k_- and k_+ calculated at 150° and 200°C from net dissolution and precipitation experiments are indeed identical within the uncertainty of the experimental method.

Values of K_{eq} for cristobalite were obtained from FOURNIER and ROWE'S (1962) dissolution data and steady state values of mSi(OH)_4 approached from supersaturated conditions measured in this study, Table 1.

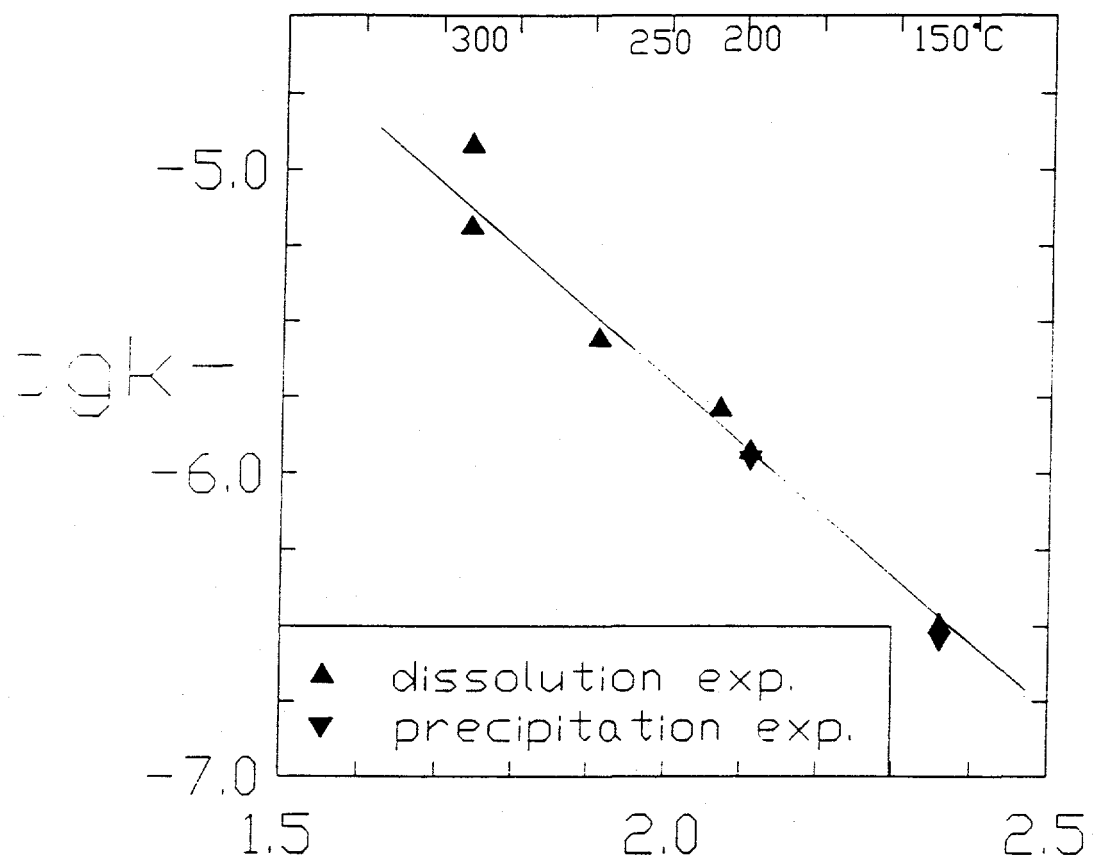


Figure 3. Arrhenius plot of $\log k$ vs $1000/(T \text{ K})$ for the reaction, $\text{SiO}_2, \text{xtb} + 2\text{H}_2\text{O}_1 = \text{Si}(\text{OH})_4, \text{aq}$, from 150° to 300°C . The energy of activation " E_a " derived from the slope of the curve is $50.0^{+/-2.4} \text{ kJ}\cdot\text{mol}^{-1}$.

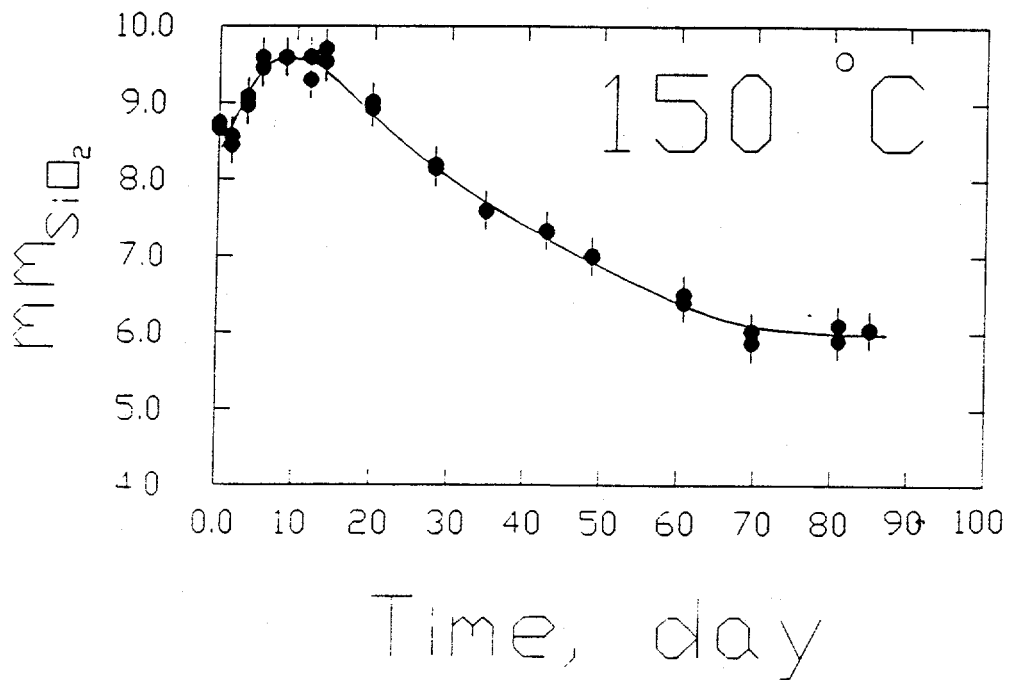


Figure 4. Precipitation of silica from aqueous solution at 150°C on crystalline cristobalite seed material. Two samples were taken at each sampling interval. The vertical line associated with each solid circle represents a 5% variation in analysis of a 10.0 mm SiO₂ measured concentration.

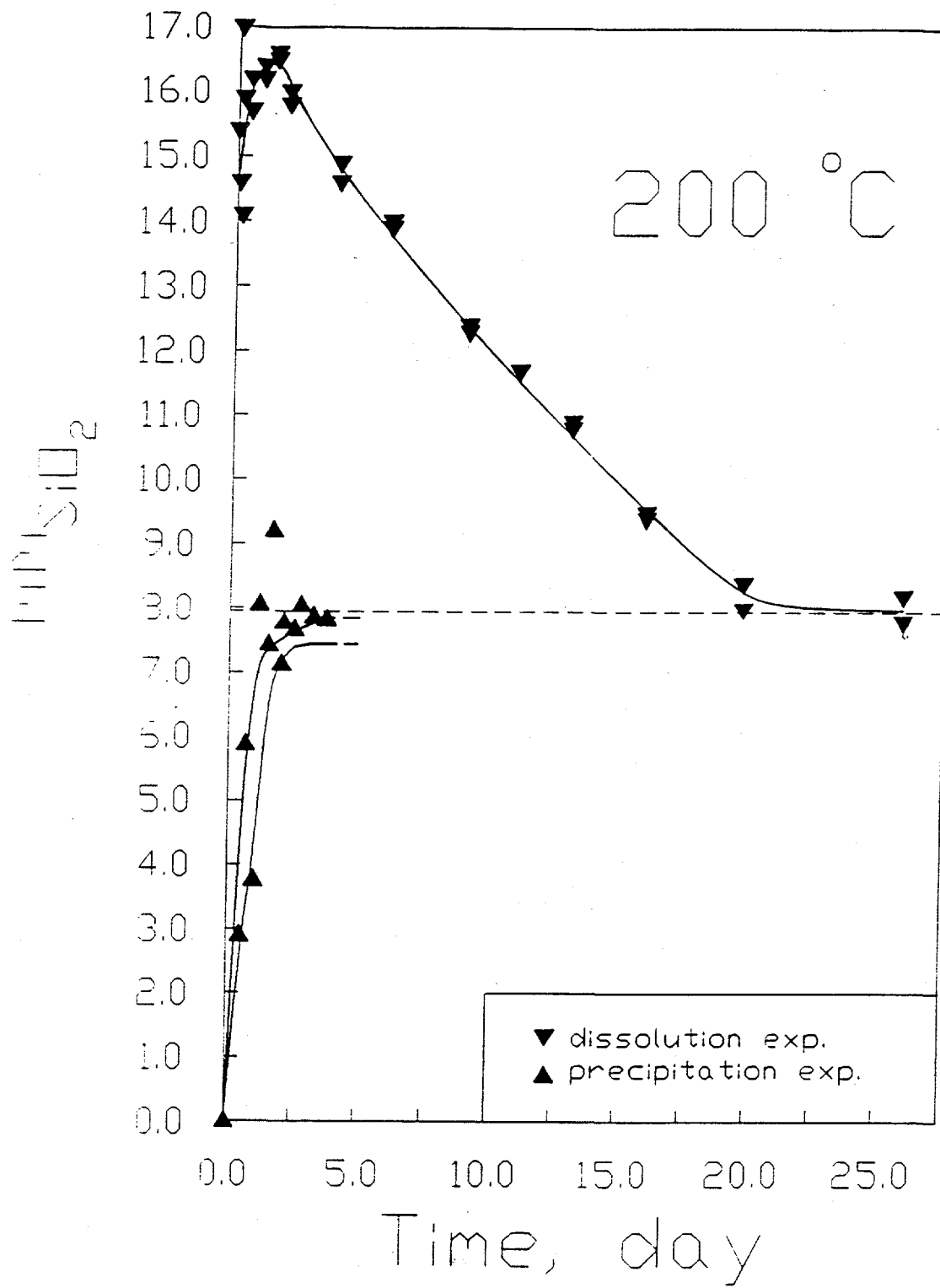


Figure 5. Precipitation of silica from aqueous solution at 200°C on crystalline cristobalite seed material. Two samples were taken at each sampling interval. The vertical line associated with each solid circle represents a 5% variation in analysis of a 10.0 $\text{mm} \text{SiO}_2$ measured concentration.

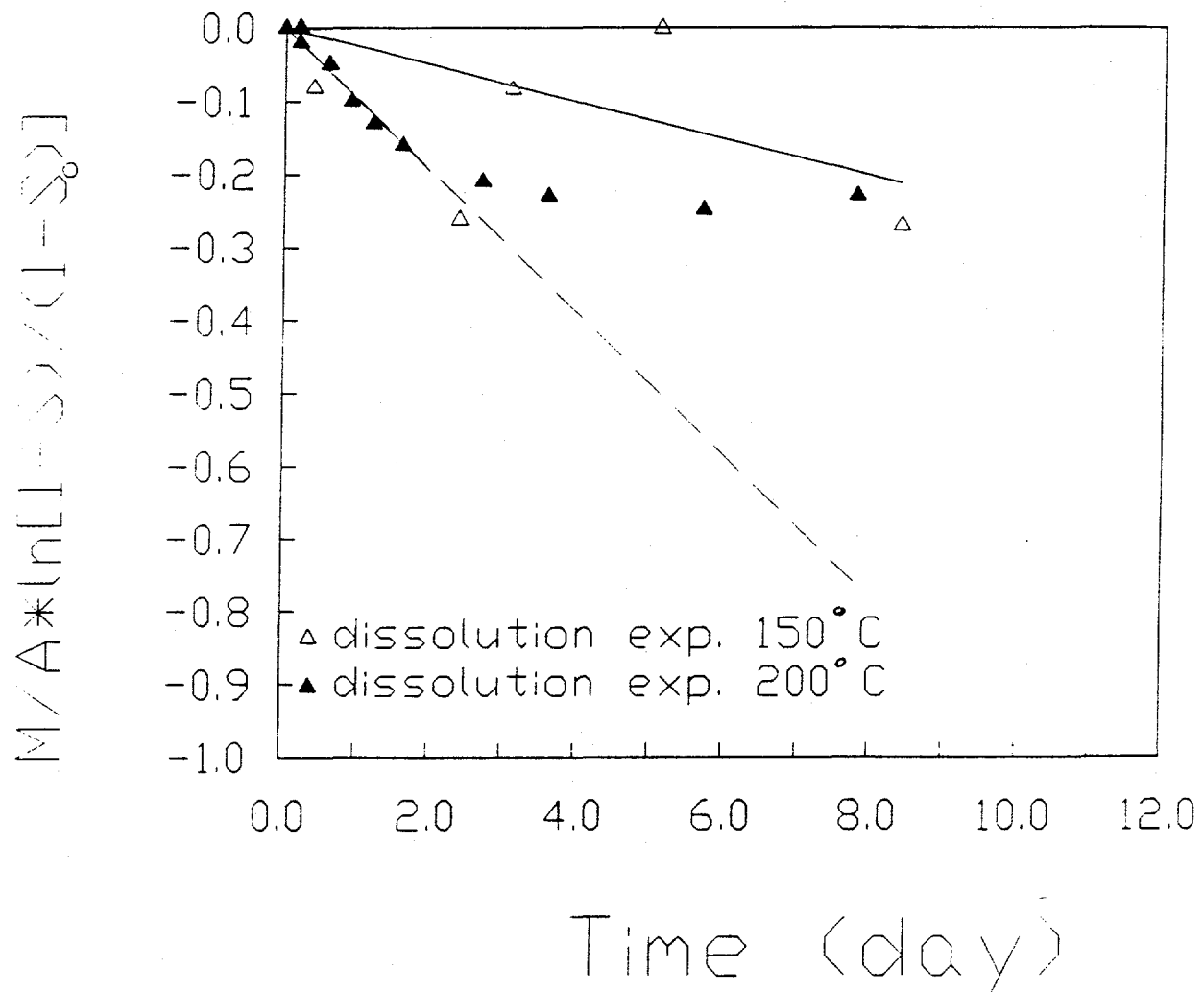


Figure 6. Regression of the rate vs. time data for dissolution experiments from 150° and 200°C. The solid and dashed lines reflect the data regressed in determining k_{+-} . As the measured aqueous silica concentrations approached steady state conditions the relative uncertainties in the plotted data are greatly magnified.

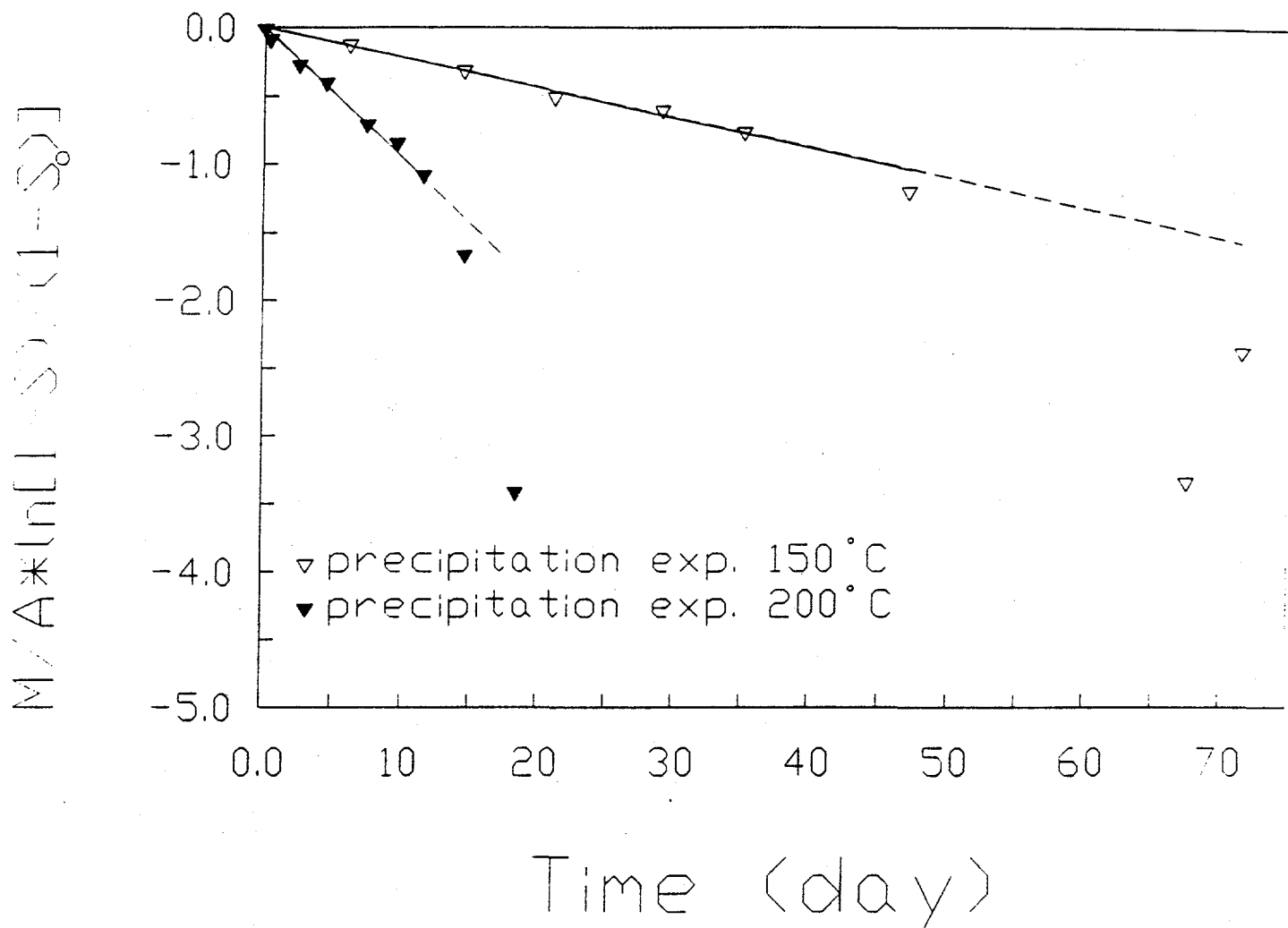


Figure 7. Regression of the rate vs. time data for precipitation experiments from 150° and 200°C. The solid and dashed lines reflect the data regressed in determining $K_{4+/-}$. As the measured aqueous silica concentrations approached steady state conditions the relative uncertainties in the plotted data are greatly magnified.

Discussion

The initial kinetic experiments were carried out under three phase conditions, cristobalite seed and two fluid H_2O phases, in a rocking autoclave. This classical experimental approach has been used extensively to determine the solubility and kinetics of different silica phases. A problem which randomly occurred with this experimental approach, at this and one other laboratory, was the precipitation of amorphous silica along the liquid, vapour, autoclave join.

The presence of silica precipitated on the interior autoclave walls was readily observed and data from those experiments were rejected. What was more difficult to determine, if it indeed occurred, was the precipitation of a second silica phase amongst the starting seed material. The initial dissolution experimental results suggested that the precipitation of a second silica polymorph did occur due to reduced net dissolution rates as silica concentrations exceeded $mSi(OH)_4,_{qtz}$. For these three phase experiments only the dissolution data for $mSi(OH)_4$ less than $mSi(OH)_4,_{qtz}$ were used. While within the above constraints the rocking autoclave dissolution kinetic data was valid, the attendant problems were bothersome and precluded the direct measurement of precipitation data.

By altering the experimental procedure to include only two

phases, cristobalite and liquid H_2O , a number of advantages were realized with minimal increase in experimental complexity. The experimentally unconstrained reaction time during heating of the autoclave was greatly reduced.

Amorphous silica nucleation along the autoclave- H_2O_v - H_2O_l join was no longer possible. Silica dissolution rate data were continuous for $m_{Si(OH)_4}$ greater than $m_{Si(OH)_4,qtz}$ and silica concentrations smoothly approached a reversible steady state condition from under and over saturated conditions, Fig 5. These results suggested that the aqueous liquid-vapour-autoclave join, facilitated the nucleation of quartz and not the cristobalite seed material and as a consequence cristobalite precipitation constants were being reliably measured in the two phase system.

Under the experimental conditions of this study, 150° to 300°C and pressures less than 165 bars, cristobalite is not thermodynamically stable. To determine that cristobalite was the dominant silica polymorph present by the end of each experiment, a powder x-ray diffraction pattern was obtained of the used seed material.

While an XRD pattern will not normally detect crystalline phases present at less than 5% of the total sample mass this sensitivity can be seen to be sufficient by referring to the 200°C cristobalite precipitation experimental data. Knowing M , a calculation of the net mass of silica precipitated over the length of the experiment results in an increased seed

mass of 13%. The gross rate of cristobalite dissolution during this experiment can also be calculated,

$$\frac{dm_+}{dt} = \frac{A}{M} k_+ \quad (8)$$

at 200°C this is 10^{-4} kg/day or 10% by weight per day of the seed material. Thus it can be seen that the actual fraction of hydrothermally precipitated silica must be at least 13% and may well be greater. If the hydrothermally grown phase were quartz, with its sharp main diffraction peaks, these peaks certainly would have been observable on the XRD patterns. This type of argument supports the assertian that significant precipitation of quartz did not occur during the precipitation experiments.

During the 200°C precipitation experiment a number of sub millimetre sized highly porous silica spheres were observed in the autoclave at the end of the experiment. A single crystal x-ray scan of these spheres did not result in an identifiable pattern, again it seems likely that if these spheres were quartz the main diffraction lines for quartz would have been detectable.

The final silica concentration of the aqueous phase in equilibrium with these spheres was well below saturation values expected for solutions buffered by amorphous silica and had decreased to values identical to those determined

from cristobalite buffered dissolution experiments. Thus the precipitation of small, porous spheres of truly amorphous silica also seems an unlikely explanation.

It seems most likely that the spheres were cryptocrystalline cristobalite (opal CT) which may not exhibit a diffraction pattern and does occur naturally as spheroids, JONES et al., (1964). Opal is also associated with hydrothermal systems having silica supersaturated (with respect to quartz) aqueous fluids.

Examination of dm/dt curves for precipitation experiments at 150° and 200°C, Figs. 4 and 5, identifies an initial period where the aqueous silica concentration actually increased despite cristobalite being the only silica polymorph present and initial silica concentrations being double those determined as dm/dt approached zero.

Having previously removed ultrafine particles and not expecting the measured surface reaction to be dependent on surface morphology, BLUM et al., (1989) and MACINNIS and BRANTLY (1992), this initial observed increase in silica must reflect the presence of a limited amount of higher energy solid silica. The source of this high energy silica phase material may have been generated from the cristobalite seed during the rather violent filling of the autoclave with the aqueous silica solution or introduced from the reservoir which was contained coarse fragments of amorphous silica.

In either case, the period of increasing silica then corresponds to the time necessary to completely dissolve this high energy material.

Once dm/dt data became negative precipitation rate constants were determined and found to be in excellent agreement with rate constants determined from dissolution experiments.

The bracketed steady state cristobalite buffered conditions observed from the 200°C experiments were identical to those determined from dissolution experiments by FOURNIER and ROWE (1962). At 150°C the dm/dt precipitation data approached zero for an m_{SiO_2} of approximately 6.0 mm. This value is significantly higher than that determined by FOURNIER and ROWE (1962), 4.4 mm. The reason for this discrepancy is probably due to the range in crystallinity possible for cristoballite. The precipitation rate constants presented in Table 1 were based on the saturation values determined from our 150° and 200°C precipitation data. For the dissolution experiments the final $m_{Si(OH)_4}$ resulted from equilibrium with cristobalite which was prepared in a manner similar to that described by FOURNIER and ROWE (1962) and therefore their saturation data was used.

Conclusions

1. The energy of activation for the precipitation of cristobalite is consistent with values determined for the precipitation of quartz and amorphous silica. The

assumption that all silica polymorphs precipitate along the same rate limiting elementary reaction coordinate is confirmed.

2. The presence of cristobalite will cause the metastable precipitation of hydrothermal cristobalite resulting in suspect temperatures when the quartz geothermometer is used in cristobalite bearing terrains.

REFERENCES

AAGAARD P. and HELGESON H.C. (1982) Thermodynamic and kinetic constraints on reaction rates among minerals and aqueous solutions. I. Theoretical considerations. *Amer. J. Sci.* **282**, 237-285.

BIRD G., BOON J., and STONE T. (1986) Silica transport during steam injection into oil sands. I. Dissolution and precipitation kinetics of quartz: New results and review of existing data. *Chemical Geology*, **54**, 69-80.

BLUM A.E., YUND R.A., and LASAGA A.C. (1989) The effect of dislocation density on the dissolution rate of quartz. *Geochim. Cosmochim. Acta*. **54**, 283-297.

DOVE P.M. and CRERAR D.A. (1990) Kinetics of quartz dissolution in electrolyte solutions using a hydrothermal mixed flow reactor. *Geochim. Cosmochim. Acta*. **54**, 955-969.

DOVE P.M. and ELSTON S.F. (1992) Dissolution kinetics of quartz in sodium chloride solutions: Analysis of existing data and a rate model for 25°C. *Geochim. Cosmochim. Acta*. **56**, 4147-4156.

FLEMING B.A. (1986) Kinetics of reaction between silic acid and amorphous silica surfaces in NaCl solutions. *J Colloid Interface Sci.* **110**, 40-64.

FOURNIER R.O. (1973) Silica in thermal waters: Laboratory and field investigations. In *Proc. Int. Symp. on Hydrogeochemistry and Biogeochemistry*, Tokyo, 1970, Volume I-Hydrochemistry. Clark, Washington D.C., pp. 122-139.

FOURNIER R.O. and ROWE J.J. (1962) The solubility of cristobalite along the three-phase curve, gas plus liquid plus cristobalite. *Am. Min.* **47**, 897-903.

JONES J.B., SANDERS J.V. and SEGNIT E.R. (1964) Structure of Opal. *Nature* **204**, 990-991.

KNAUSS K.G. and WOLERY T.J. (1988) The dissolution kinetics of quartz as a function of pH and time at 70°C. *Geochim. Cosmochim. Acta*. **52**, 43-53.

LASAGA A.C. and GIBBS G.V. (1990) Ab-initio quantum mechanical calculations of water-rock interactions: Adsorption and hydrolysis reactions. *Amer. J. Sci.* **290**, 263-295.

RIMSTIDT J.D. and BARNES H.L. (1980) The kinetics of silica-

water reactions. Geochim. Cosmochim. Acta. 44, 1683-1699.

DISCLAIMER

This report was prepared as an account of work sponsored by an agency of the United States Government. Neither the United States Government nor any agency thereof, nor any of their employees, makes any warranty, express or implied, or assumes any legal liability or responsibility for the accuracy, completeness, or usefulness of any information, apparatus, product, or process disclosed, or represents that its use would not infringe privately owned rights. Reference herein to any specific commercial product, process, or service by trade name, trademark, manufacturer, or otherwise does not necessarily constitute or imply its endorsement, recommendation, or favoring by the United States Government or any agency thereof. The views and opinions of authors expressed herein do not necessarily state or reflect those of the United States Government or any agency thereof.